



FIV2018-125

NUMERICAL MODELS FOR INTERNAL SOUND PRESSURE LEVEL PREDICTION

Luca Fenini

Department of Civil and Environmental Engineering
Polytechnic University of Milan
Milan, Italy
luca.fenini@polimi.it

Stefano Malavasi

Department of Civil and Environmental Engineering
Polytechnic University of Milan
Milan, Italy
stefano.malavasi@polimi.it

ABSTRACT

In this work the noise produced by a perforated plate (orifice) inside a pipe is predicted through a numerical hybrid approach for Computational Aero-Acoustics based on the resolution of different acoustic propagation equations APE coupled with fluid-dynamic simulations and synthetic generation of the turbulent fluctuations. The objective is the study of the fluid-dynamic and the noise generation mechanisms of jets (and their reciprocal interaction) for application on more complex flow-control devices. Under the assumption of isentropic flow, a system of equations APE for acoustic pressure and acoustic particle velocity can be derived as one of the most accurate model for taking into account the convection and the refraction of the acoustic wave due to the mean sheared flow. The results are compared with the ones obtained from other APE formulations (derived with additional assumptions or with different models for the source term) and from LES direct simulations. The comparisons between different APE formulations reveals the incidence of refraction and convection on the sound pressure level inside the pipeline. On the other hand, the LES can be considered as a reference for the calibration of the numerical models for such an application.

NOMENCLATURE

- $\bar{(\cdot)}$ Time average of a quantity
- $(\cdot)_a$ Acoustic fluctuation of a quantity
- $(\cdot)_t$ Turbulent fluctuation of a quantity
- p Pressure field
- ρ Density field
- \mathbf{u} Velocity field
- γ Specific heat ratio
- D Pipe diameter
- d Orifice diameter
- t Orifice thickness
- Re_D Reynolds number referred to pipe diameter
- M_j Jet Mach number

INTRODUCTION

The generation of aerodynamic noise is a very common phenomenon that occurs in several fields and applications such as wind turbines, HVAC systems, automotive and pipelines. The location and characterization of the source of noise inside ducts is a demanding process whose complexity is due to the propagation of the sound inside the pipes and to the presence of singularities as bends, cavities and control valves. Flow control devices are usually installed in order to induce a pressure drop that on turn leads to a loss of energy and to its conversion

into heat and noise.

Most of the times a control valve perturbs the flow deviating it into different paths that, at their outlet, create different interacting jets. For a good prediction of their acoustic emission is thus important to be able to predict the noise generated by a jet. In literature, the acoustic emission of a free jet has been studied as a benchmark for the noise produced by a sheared flow both with a theoretical-experimental approach [1] [2] [3] and with numerical simulations [4] [5].

Confined jets has been studied by Kirkwood [6] who carried out experimental analysis on the noise emitted by different perforated plates analysing the influence of the number, the diameter and the thickness of perforations.

Here we are interested in the comparison of the results coming from different numerical models in order to define the advantages of each method. In particular we want to analyse the efficiency and reliability of different Acoustic Propagation Equations (APE) in the description of the noise generation mechanism and in its intensity prediction. This is done on a perforated plate (orifice) installed inside a circular pipe.

MODELS FOR NOISE PREDICTION

The production of aerodynamic noise is a complex mechanism that is usually localized in a small region (source region) outside of which the acoustic waves are just propagated without any further production of noise. Inside pipes the source region is always close to a singularity that perturbs the flow. The evaluation of the acoustic power of such a source can be performed by numerical simulations in the near-field (domain close to the source region) with direct approaches as DNS (Direct Numerical Simulation) or LES (Large Eddy Simulation). DNS requires a domain discretization so fine that most of the times it is too much time-demanding, while LES allows to save computational time working with less degrees of freedom.

An alternative approach for CAA (Computational AeroAcoustics) is represented by the hybrid methods that solve the flow field and the acoustic one in two different steps dealing respectively with the generation and the propagation of the noise in the domain. Acoustic analogies from Lighthill (1952), Curle (1955), Lilly (1958), Ffowcs Williams (1963) and Ffowcs Williams - Hawkins (1969)

provide analytical prediction of the acoustic pressure in the far field under different assumptions. Inside pipes, anyway, the dimensions of the source region, the refraction of the mean sheared flow and the influence of walls cannot be easily described by those models. A more efficient approach consists in the resolution of Acoustic Perturbation Equations (APE) for the flow-induced acoustic field in space and time. Different formulations of APE have been developed in literature and they are based on the linearization of the mass, momentum and energy equation for inviscid flows in order to obtain a system of equations whose left-hand side corresponds to the Linearized Euler Equations (LEE), and whose right-hand side contains all the non-linear and viscous terms. The acoustic perturbations are defined as the deviation from the time-averaged quantities and from the turbulent fluctuations. Velocity field can be decomposed as

$$\mathbf{u} = \bar{\mathbf{u}} + \mathbf{u}_t + \mathbf{u}_a \quad (1)$$

where the subscript $(\cdot)_a$ means the acoustic perturbation, the symbol $(\bar{\cdot})$ the time-average and the subscript $(\cdot)_t$ the turbulent fluctuations (the same decomposition is applied to pressure and density too).

The APE momentum equation can be written as [7] [8]

$$\frac{\partial \mathbf{u}_a}{\partial t} + \bar{\mathbf{u}} \cdot \nabla \mathbf{u}_a + \mathbf{u}_a \cdot \nabla \bar{\mathbf{u}} + \frac{1}{\bar{\rho}} \nabla p_a - \frac{\rho_a}{\bar{\rho}^2} \nabla \bar{p} = \mathbf{S}_m \quad (2)$$

while the continuity equation becomes

$$\frac{\partial p_a}{\partial t} + \bar{\mathbf{u}} \cdot \nabla p_a + \gamma \bar{p} \nabla \cdot \mathbf{u}_a + \gamma p_a \nabla \cdot \bar{\mathbf{u}} + \mathbf{u}_a \cdot \nabla \bar{p} = S_p. \quad (3)$$

where γ is the specific heat ratio. During the numerical resolution of the APE, the source terms \mathbf{S}_m in Eq 2 and S_p in Eq 3 are computed from the averaged quantities and from the turbulent fluctuations of the velocity field \mathbf{u}_t . A fast computation of the source terms can be obtained with the application of a stochastic approach (SNGR) [8] that synthesizes \mathbf{u}_t at each time step receiving as input only the turbulent kinetic energy and the mean flow field.

NUMERICAL SETTINGS

Very often, at the outlet of control devices, the flow can be described as a complex combination of different

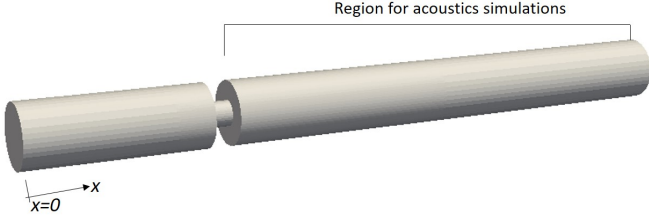


FIGURE 1: Numerical domain for simulations.

incident jets. In this work we focus on the noise produced by a circular jet generated at the outlet of a perforated plate (orifice) installed inside a 3” pipe ($D = 77.5$ mm). The orifice is characterized by a hole of $d = 30.5$ mm diameter with a thickness equal to $t = 3$ mm.

The numerical simulation is run on a three-dimensional domain with the inlet placed $10d$ upstream of the resistor and the outlet $22d$ far from the orifice (see Fig. 1). The fluid flowing inside the pipe is dry air whose properties are evaluated under the thermophysical model of ideal gas with temperature-dependent dynamic viscosity (Sutherland’s law) and specific heat described by a polynomial relationship (JANAF coefficients). The flow is imposed thanks to the definition of total pressure and static pressure respectively at the inlet ($5 \cdot 10^5$ Pa) and outlet ($4 \cdot 10^5$ Pa) of the domain. The flow is characterized by a Reynolds number (referred to the upstream conditions) equal to $Re_D = 5.3 \cdot 10^5$ and a maximum Mach number (referred to the jet velocity) equal to $M_j = 0.7$.

The LES simulation is performed on the open-source software OpenFOAM with a one-equation eddy viscosity model an run on a uniform cartesian grid with 78 cells in the radial direction that allow an accurate sound propagation for frequencies up to almost 70kHz ($f_{max} = c_0/(5\Delta x)$ [9]). Second order schemes in time and space are used. The simulation is run for about 200 characteristic periods D/U_j with an adjustable time step to maintain the Courant number lower than 0.75. Wave transmissive boundary condition at the outlet are added to avoid numerical reflection of the outgoing waves.

The evaluation of the emitted noise is performed through the RMS of the pressure fluctuations which provides information about the sound pressure level SPL

$$SPL = 20 * \log_{10} \left(\frac{P_{rms}}{2 * 10^{-5}} \right). \quad (4)$$

LES simulation can be considered as reference so-

lution for the comparison with the results obtained from different formulations of APE. Even though these equations are less accurate than the LES because of additional assumptions and simplifications, their application to industrial problems can be very competitive because of the lower required computational effort.

Provided that, when interested in the propagation of sound in a quiescent medium, the APE system Eq 2-Eq 3 can be rewritten as the d’Alembert equation, it is straightforward that under strong assumption the APE equations can be decoupled and the acoustic pressure can be thus evaluated with the resolution of a non-homogeneous d’Alembert equation. For instance, if we assume that the acoustic wave propagation is not affected by refraction effects, we can neglect the second and third terms in Eq 2 and obtain an equation for acoustic pressure as follows:

$$\frac{\partial^2 p_a}{\partial t^2} - c^2 \nabla^2 p_a = S \quad (5)$$

where the source term S depends on the properties of the flow (velocity and pressure). For a non-uniform field is

$$S = \frac{\partial S_p}{\partial t} - \mathbf{S}_m \cdot \nabla \bar{p} - c^2 \frac{\rho_a}{\bar{\rho}} \nabla^2 \bar{p} + \frac{1}{\bar{\rho}} \nabla p_a \cdot \nabla \bar{p} + \frac{\rho_a}{\bar{\rho}^2} \frac{\nabla \bar{p}^2}{2} - \bar{\mathbf{u}} \cdot \frac{\partial \nabla p_a}{\partial t} - \gamma \frac{\partial p_a}{\partial t} \nabla \cdot \bar{\mathbf{u}} - \gamma \bar{p} \nabla \cdot \mathbf{S}_m \quad (6)$$

where $c = \sqrt{\gamma \bar{p} / \bar{\rho}}$ is the speed of sound.

Other assumptions can be done on the source terms of the APE system Eq 2-Eq 3: S_p is usually neglected while \mathbf{S}_m has been described in different ways in literature. In this work we refer to the formulation presented in [10]:

$$\mathbf{S}_m = - \left(\mathbf{u}_t \cdot \nabla \mathbf{u}_t - \overline{\mathbf{u}_t \cdot \nabla \mathbf{u}_t} \right). \quad (7)$$

When the APE are run starting from a steady flow field, the turbulent velocity field \mathbf{u}_t is not directly available. A synthetic generation of this field is done thanks to the SNGR model that describes $\mathbf{u}_t(\mathbf{x}, t)$ as a finite sum of Fourier modes properly time-correlated (Bailly method [10]). The obtained field is used in the evaluation of the source terms Eq 7.

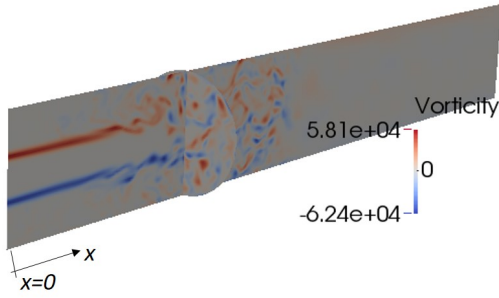


FIGURE 2: Vorticity field: components orthogonal to the visualized surfaces. Flow from left to right.

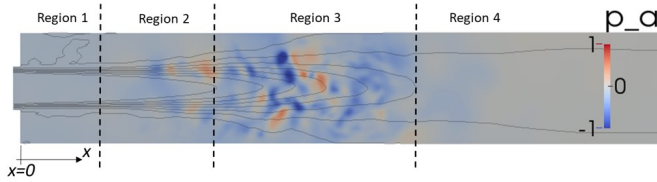


FIGURE 3: Instantaneous p_a downstream of the orifice on a longitudinal section and contours of the longitudinal mean flow velocity (LES). Scale factor $3 \cdot 10^4$.

RESULTS AND DISCUSSION

Before analysing the intensity of the predicted noise, LES simulation provides information about the localization of the source region i.e. that area characterized by high turbulence inside of which the noise generation occurs. As can be seen in Fig. 2, the instantaneous vorticity pattern on a longitudinal and transversal section of the pipe shows that the highest intensity of vorticity is located in two areas: in the shear layer ring around the potential core downstream of the orifice and in the area where the turbulence fills the pipe. Except for the very first part of the shear layer (close to the orifice) where the turbulence is low, these are exactly the areas that form the acoustic source region.

In addition to the localization of the source region we are interested in the evaluation of the noise through the analysis of the acoustic pressure field p_a . An instantaneous visualization of the acoustic pressure evaluated with LES is shown in Fig.3 with the addition of contours of the mean longitudinal velocity field for a better recognition of the different fluid-dynamic regions. The acoustic pressure is normalized because Fig.3, 5 and 6 are here analysed just for a qualitative comparison of the pattern returned by the

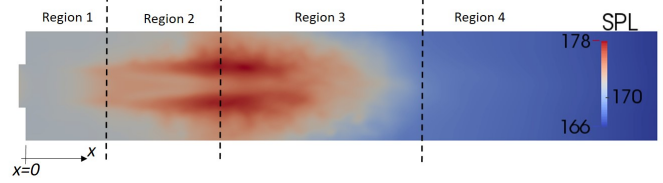


FIGURE 4: Sound pressure level downstream of the orifice on a longitudinal section of the pipe. Flow from left to right.

different numerical methods. In Fig.3 four areas can be identified: the first one is located just downstream of the orifice and here a very thin shear layer surrounds the jet's potential core. In this region, even if the vorticity is high (see Fig.2), the noise production is low. In the second region the shear layer grows and actively participates in the noise generation process. This region is characterized by the presence of alternate structures of low and high acoustic pressure that are generated by the interaction of the acoustic wave with the flow field. The generated sound is then convected downstream and its intensity grows up to reach a peak in the third region where the turbulence fills the pipe and the jet's potential core is no longer present (see the transverse section in Fig.2). Moving downstream, in the fourth area the turbulence intensity decreases so much that its noise production is negligible and the acoustic wave is just propagated through the pipe.

From the RMS of the acoustic pressure the sound pressure level pattern visualized in Fig. 4 is computed: the highest intensities are located around the shear layer in the second region and in the first part of the third area.

The LES results can be considered a reference for the comparison with the results coming from different APE formulations. Since the APEs solve only the acoustic propagation, they need information about mean quantities (turbulent kinetic energy, velocity, pressure and density) which in this work are obtained from a time-average applied on the LES output. Figure 5 displays the pattern of the instantaneous acoustic pressure (normalized because p_a pattern is shown just for qualitative comparisons) returned by the APE system Eq 2-Eq 3. In the second region previously identified in Fig.3, the alternate structures of low and high pressure are here more defined than in the LES output while in the third region they are fast dissipated.

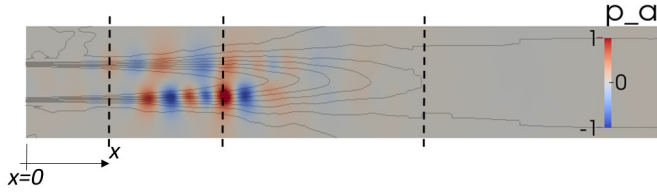


FIGURE 5: Instantaneous p_a obtained with the APE Eq 2-Eq 3 with the source term Eq 7. Scale factor $5 \cdot 10^5$.

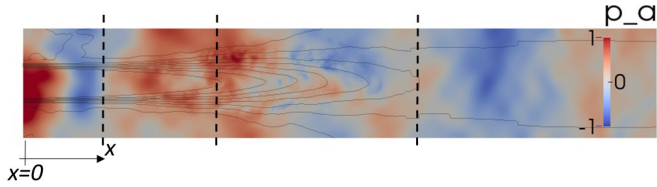


FIGURE 6: Instantaneous p_a obtained with the APE Eq 5. Scale factor $2.5 \cdot 10^4$.

On the contrary, the APE Eq 5 do not take into account the refraction effects of the acoustic wave with the sheared mean flow because in their momentum equation the second and third terms in Eq 2 are neglected. The effect of this change in the set of the solved equations is straightforward when the acoustic pressure pattern displayed in Fig.6 is compared with the ones previously shown in Fig.3 and 5: in the second region, the alternate structures of high and low values of acoustic pressure are not caught by the APE Eq 5. Since the only difference in the compared APE models is connected to the refraction terms, the production mechanism of the aerodynamic noise in a confined jet is thus clearly influenced by the refraction effects of the mean flow field on the acoustic wave.

Besides the understanding of the mechanism of noise generation and propagation, a quantitative analysis on the APE results can be conducted evaluating the intensity of the returned noise. Figure 7 shows the trend of the sound pressure level on the walls of the pipe downstream of the orifice obtained with different models (with LES, APE system Eq 2-Eq 3 and modified APE Eq 5). The LES curve has a peak of noise of 175 dB placed at $5d$ downstream of the orifice while the one computed with the APE Eq 2-Eq 3 has 1 dB lower intensity but is slightly moved upstream (at $4d$). These distances from the orifice

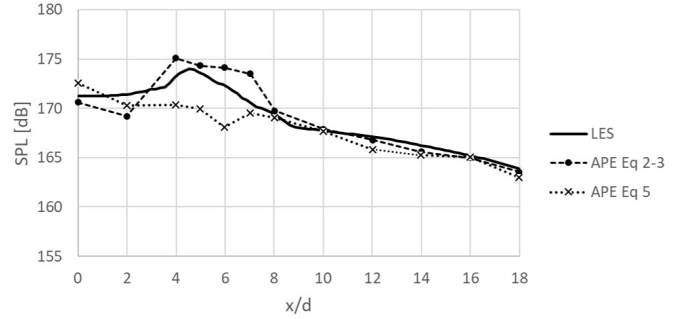


FIGURE 7: SPL along the pipe's walls downstream of the orifice: APE from LES-averaged flow field. Sampling every $2d$ except for the $5d$ probe which is the distance of the LES peak from the orifice.

correspond to the transition between the second and third region previously introduced.

The APE Eq 5 on the contrary is not able to describe the peak of the SPL since it is related to the local increase of noise in the second and third region; the SPL is so underestimated of about 5 dB.

On the contrary, moving in the fourth region far from the source of noise, all the described models return almost the same values of SPL with a maximum difference of 1 dB.

Further comparisons can be developed on the resolution of the APE run from a steady flow field obtained with a compressible RANS simulation (with the same boundary conditions as the LES simulation). Due to the use of closure models (here $RNG\kappa - \varepsilon$ model is adopted), the mean flow obtained with RANS is affected by some differences respect to the averaged one from LES. Even though these differences are not involved in the mechanism of the noise generation and propagation, they act on the localization of the SPL peaks (jet length is not equal) and on the amplitude of the acoustic pressure (and of the SPL). Figure 8 shows that the SPL curve returned by the APE has a peak located $6d$ downstream of the orifice whose intensity is 2.3 dB lower than the one computed with the APE applied to the LES averaged fields. The shift of the peak is expected since the jet core predicted by the RANS is longer and this implies that the source region is moved more downstream than in the LES. On the contrary, the difference in the intensity of the SPL peak is probably connected to errors introduced by the closure models used for the description of the turbulence. The acoustic power of the source region is underestimated

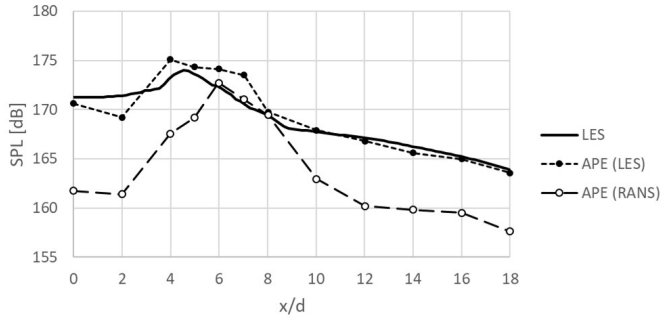


FIGURE 8: SPL along the pipe’s walls downstream of the orifice: APE from LES-averaged flow field and from the RANS mean flow. Sampling every $2d$ except for the $5d$ which is the distance of the LES peak from the orifice.

and this is even more relevant far from the source region where the predicted SPL is about 5 dB lower than the one predicted from the LES output.

CONCLUSIONS

In this work we have studied the acoustic emission of a confined jet with different numerical methods. A direct evaluation of the noise from LES has been compared with the results coming from different formulation of APE obtained changing the momentum equation and the definition of the mean flow field used as initial condition for the acoustic simulations.

It has been found that, for a good description of the noise generation mechanism, the complete form of APE must be used because simplified formulations do not take into account the refractive effects.

The comparison between the noise directly predicted by LES and the one by APE (applied to LES output) has shown that the APE return a distribution of the noise along the pipe’s walls that is in accordance with the LES result since the SPL maxima differ for just 1 dB even though the peak position is shifted $1d$ upstream respect to LES prediction.

On the other hand, when APE are applied to the mean flow field obtained from RANS, they underestimate the noise along all the pip probably because of the RANS turbulence models. The position of the peak is shifted according to the differences between the LES averaged flow and the RANS mean one.

Finally, when interested only in the SPL inside the pipe far from the source region, all the tested APE models

(applied to LES flow field) fit the noise computed with LES. On the contrary, the RANS+APE approach underestimates it of about 5 dB.

Further analysis should be conducted on the influence of the turbulence model on the final prediction.

ACKNOWLEDGEMENTS

Grateful acknowledgements are due to Pibiviesse S.r.l that supports our activities and to F.C. Bossi for his previous work in this research group.

REFERENCES

- [1] M. J. Lighthill, 1952 “On sound generated aerodynamically, I. General theory” *Proc. Roy. Soc.*, **A 211**, 564-587
- [2] M. J. Lighthill, 1953 “On sound generated aerodynamically, II. Turbulence as a source of sound” *Proc. Roy. Soc.*, **A 222**, 1-32
- [3] M. J. Lighthill, 1963 “Jet Noise” *AIAA Journal*, **1(7)**, 1507-1517.
- [4] J. Freund, 2001 “Noise sources in a low-Reynolds-number turbulent jet at Mach 0.9” *Journal of Fluid Mechanics*, **438**, 277-305
- [5] C. Bogey, C. Bailly, D. Juve, 2000 “Computation of the sound radiated by a 3-D jet using Large Eddy Simulation” *6th AIAA/CEAS Aeroacoustics Conference*, No. 2009 in AIAA 2000
- [6] A. D. Kirkwood, 1992 “Aerodynamic Noise Generation in Control Valves” *Ph.D. Thesis*, University of Manchester
- [7] R. Ewert, W. Schroder, 2003 “Acoustic Perturbation Equations based on flow decomposition via source filtering” *Journal of Computational Physics*, **188** (2), 365-398
- [8] W. Bechara et Al, 1994 “Stochastic Approach to Noise Modeling for Free Turbulent Flows” *AIAA Journal*, **32** (2), 455-463
- [9] C. Bogey, C. Bailly, D. Juve, 2003 “Noise Investigation of a High Subsonic, Moderate Reynolds Number Jet Using a Compressible Large Eddy Simulation” *Theoret. Comput. Fluid Dynamics*, **16**, 273297
- [10] C. Bailly, P. Lafon, S. Candel, 1995 “A stochastic approach to compute noise generation and radiation of free turbulent flows” *AIAA/CEAS Aeroacoustic Conference*